Reducing discrepancies between 3D and 2D simulations due to cell packing density

Clegg, Robert; Kreft, Jan-Ulrich

DOI:
10.1016/j.jtbi.2017.04.016

Document Version
Peer reviewed version

Citation for published version (Harvard):
Clegg, R & Kreft, J-U 2017, 'Reducing discrepancies between 3D and 2D simulations due to cell packing density', *Journal of Theoretical Biology*, vol. 423, pp. 26-30. https://doi.org/10.1016/j.jtbi.2017.04.016

Reducing discrepancies between 3D and 2D simulations due to cell packing density

Robert J Clegg , Jan-Ulrich Kreft

PII: S0022-5193(17)30180-7
DOI: 10.1016/j.jtbi.2017.04.016
Reference: YJTBI 9041

To appear in: *Journal of Theoretical Biology*

Received date: 22 June 2016
Revised date: 11 April 2017
Accepted date: 13 April 2017

Please cite this article as: Robert J Clegg , Jan-Ulrich Kreft , Reducing discrepancies between 3D and 2D simulations due to cell packing density, *Journal of Theoretical Biology* (2017), doi: 10.1016/j.jtbi.2017.04.016

Highlights

- A discrepancy between 2D/3D simulations of particles arises due to packing densities.
- The discrepancy affects simulations of biofilms.
- Two methods are proposed which greatly reduced this issue.
- These findings will be relevant to many other particle- or cell-based models.

Reducing discrepancies between 3D and 2D simulations due to cell packing density

Robert J Clegg[1*], Jan-Ulrich Kreft[1]

[1]Centre for Computational Biology, Institute of Microbiology and Infection, School of Biosciences; University of Birmingham, Edgbaston, Birmingham B12 5TT, United Kingdom

[*]**Correspondence:** Robert Clegg, Centre for Computational Biology, Haworth Building, University of Birmingham, Edgbaston, Birmingham B12 5TT, United Kingdom[†]
r.j.clegg@bham.ac.uk

Keywords: individual-based model, agent-based model, spatial structure, biofilm, heuristics

[†] Current address: Tessella, 26 The Quadrant, Abingdon Science Park, Abingdon, Oxfordshire, OX14 3YS, United Kingdom
roughhawkbit@gmail.com

Abstract

Modelling all three spatial dimensions is often much more computationally expensive than modelling a two-dimensional simplification of the same system. Researchers comparing these approaches in individual-based models of microbial biofilms report quantitative, but not qualitative, differences between 2D and 3D simulations. We show that a large part of the discrepancy is due to the different space packing densities of circles versus spheres, and demonstrate methods to compensate for this: the internal density of individuals or the distances between them can be scaled. This result is likely to be useful in similar models, such as smoothed particle hydrodynamics.

Letter

Simplification of the mental model one has of a real-life system is practically unavoidable when translating that mental model into a mathematical model: simpler models tend to be more analytically tractable or less computationally expensive. This is particularly true when the system belongs to biology (Gunawardena, 2014). A typical example of model simplification is using fewer spatial dimensions than the realistic three. This is justified when some dimensions may be considered as equivalent to each other, and when there is no need to consider navigation of fluids or objects around obstacles. Relevant examples where reduced dimensionality is assumed include smooth particle hydrodynamics of viscous media (Lu et al., 2005) and Monte Carlo simulations of protein interactions (Woodard et al., 2016).

While such simplification of a model is useful, it can introduce bias and so affect results. Bacterial cells are often modelled as hard spheres (three-dimensional) or hard circles (two-dimensional). We show that a bias is introduced when simplifying a model of spheres to a model of circles, which does affect results in simulations of biofilm growth and may also

affect simulations of other systems. A method to compensate for the bias is developed from first principles and its efficacy demonstrated in biofilm simulations.

Biofilms are communities of microorganisms growing in close proximity, attached to some solid surface or interface, and are important habitats in the study of microbial ecology and for microbes themselves (Allison and Gilbert, 1992; Costerton et al., 1995). Microorganisms in aqueous biofilms consume nutrients dissolved in the fluid, grow and reproduce, and so cause the expansion of the entire community. Dissolved nutrients and other chemicals are typically referred to as solutes. Fluid flow is obstructed within the biofilm and its immediate surroundings so much that the motion of solutes is dominated by diffusion and advection can be ignored (Manz et al., 2003; Neu et al., 2010).

The two dimensions parallel to the solid surface are often considered equivalent, since the concentration gradient is typically strongest along the axis orthogonal to the surface and the gradient primarily determines biofilm morphology. In the previous studies on biofilm simulation referenced in this work, the key focus is often the qualitative, emergent behaviour of microbial populations rather than quantitatively precise prediction of biofilm growth. Other systems may be translationally invariant along one dimension, such as the azimuthal when considering flow along a pipe.

A toy model of biofilm growth (single solute and single biomass type) illustrates the key processes. The diffusion-reaction equation describes the dynamics of solute concentration:

$$\frac{\partial c}{\partial t} = \nabla \cdot (D \nabla c) + f(c, X) \tag{1}$$

where c is the solute concentration, D the diffusivity, X the biomass concentration, and function f the combined rates of production (positive) and of consumption (negative) by chemical reactions (Wanner et al., 2006; Horn and Lackner, 2014). In the simulations

reported later, diffusion-reaction is assumed to operate on a far shorter timescale than growth, and so the former is taken to be at steady-state when the latter is considered: in the context of Equation (1), this means that the time-derivative on the left-hand side is set to zero (Lardon et al., 2011).

The distribution of biomass is given in more general terms:

$$\frac{\partial X}{dt} = growth(c, X) + movement(X). \quad (2)$$

The *growth* term is linked to the reactions described by function *f* in (1), and the *movement* term depends on further details of the model. The exact forms of functions *f*, *growth* and *movement* used in simulations here are described in **Supplementary File 1.** Numerical solution of (1) and (2) may require spatial discretisation of continuous fields, e.g., into rectilinear grids.

Individual-based modelling has proven a popular method of investigating biofilms, particularly since the heterogeneity within clonal populations of microorganisms became apparent (Kreft et al., 2013; Ackermann and Schreiber, 2015; Hellweger et al., 2016). Of these, hybrid models are among the most realistic; these treat microorganisms as discrete, non-overlapping particles, and solutes as continuous scalar fields. The rule that particles may not overlap leads to the *movement* part of (2), since cells push away their neighbours as they grow and divide (Kreft et al., 1998). The biomass concentration field and/or field for reaction rates must be updated at each time step by mapping the biomass and/or reaction rates of each microbial cell onto the grid voxel(s) corresponding to its location. Particles have internal biomass density, ρ, and fill the space with packing density, η. In a grid voxel $\boldsymbol{i}$, the fraction of space occupied by biomass is described by $\eta_i \in [0, 1]$ and the fraction that is fluid is therefore given by $(1-\eta_i)$: this is also known as the porosity. The local biomass concentration is then $X_i = \rho\ \eta_i$.

Individual microbial cells are often represented as hard spheres in three-dimensional space and as hard circles in two-dimensional space (Figure 1A,B). Where physically realistic parameters (e.g. density as mass per volume) require inclusion of an extrusive third dimension, circles are typically extended to cylinders with co-parallel axes of identical length (Picioreanu et al., 1998a, 1998b ; Alpkvist et al., 2006; Lardon et al., 2011; Ardré et al., 2015). Furthermore, the thresholds in cell radius that trigger events such as division and death are consistent between simulations in 2D and in 3D: if thresholds of volume or mass were used, the cell radii at these events would vary according to the length of this third dimension (Lardon et al., 2011). In two-dimensional simulations this approach ensures that cell radii, and so the overall shape and size of the biofilm, are unaffected by the choice of extrusion thickness. Where these simplifications are made, and two- and three-dimensional simulations of the same system compared, authors observe quantitative differences but little or no qualitative differences. Picioreanu et al. (2004) modelled a multispecies nitrifying biofilm: compared to biofilms simulated in 3D, those in 2D grew more quickly in terms of total biomass per unit surface area and caused ammonium concentrations in the bulk fluid to decline more rapidly, but the overall trends were the same. Alpkvist et al. (2006) built on the work of Picioreanu et al. (2004), expanding the model to include extracellular polymeric substance (EPS): they also reported quantitative differences that did not significantly change the conclusions, but did not describe these differences in any detail.

We point to the different packing densities of circles and of spheres as the source of these quantitative differences. The maximal packing density of spheres of equal radius is

$$\eta_{sphere} = \frac{\pi}{3\sqrt{2}} \approx 0.74 \qquad (3)$$

(Hales, 1992) and the equivalent packing density for circles is

$$\eta_{circle} = \frac{\pi}{2\sqrt{3}} \approx 0.91 \quad (4)$$

(Tóth, 1972). Given that simulated cells in a biofilm are growing, they will have different radii and are unlikely to achieve optimal packing. However, the packing achieved by random close-packed circles and spheres fall short of the maximum packing by a similar degree in two- and in three-dimensional simulations:

$$\hat{\eta}_{sphere} \approx 0.64 \quad (5)$$

$$\hat{\eta}_{circle} \approx 0.82 \quad (6)$$

(Visscher and Bolsterli, 1972; Berryman, 1983).

Because of this, we expect the concentration in the biomass grid to be higher in two-dimensional simulations, leading to steeper solute gradients. The overall height of the biofilm is also likely to be reduced, an outcome of interest to those using these models for prediction of specific systems.

To compensate for this discrepancy, we propose to scale the internal biomass density of simulated cells, ρ, as a convenient solution. Following (3) and (4), we define a new internal biomass density, ρ_2, for 2D simulations:

$$\rho_2 = \frac{\eta_{sphere}}{\eta_{circle}}\rho = \sqrt{\frac{2}{3}}\rho \approx 0.82\rho. \quad (7)$$

There are no biological implications of this rescaling, unless any processes are modelled that depend explicitly/directly on density.

Results of simulations in iDynoMiCS (Lardon et al., 2011) confirm that adopting this approach produces more similar biofilm structures between simulating with three and two dimensions (Figure 2A-C). Compared with 2D simulations where the internal biomass density is the same, adopting ρ_2 results in (1) the maximum biofilm thickness increasing at a

more similar rate (Figure 2A), (2) position within the biofilm having a more similar effect on specific growth rate of individuals (Figure 2B), and (3) the overall biomass concentration being more similar as a function of position within the biofilm (Figure 2C) to that of an equivalent 3D simulation.

However, iDynoMiCS did not resolve all overlaps between cells completely due to limited iterations and tolerance settings in these simulations. An opportunity arises to scale another parameter instead: in each time step, iDynoMiCS's shoving algorithm attempts to eliminate any overlap between microbial cells due to growth, etc. However, it is computationally expensive to ensure that all cell surfaces touch exactly. So, for the purposes of the shoving algorithm, the radii of cells are scaled by a "shove factor" (Figure 3). The value of this shove factor, s_f, is chosen heuristically; values of around 1.05 or 1.10 are typical.

Taking the shove factor in three-dimensional simulations to be $s_{f,3}$ and keeping the internal biomass density ρ fixed, we can then calculate an equivalent shove factor in 2D simulations:

$$s_{f,2} = \sqrt{\left(s_{f,3}\right)^3 \frac{\eta_{circle}}{\eta_{sphere}}} = \left(s_{f,3}\right)^{3/2} \left(\frac{3}{2}\right)^{1/4}. \quad (8)$$

A 3D shove factor, $s_{f,3}$, of 1.05 then corresponds to a $s_{f,2}$ of approximately 1.19. Figure 2D-F compares the results of scaling the shove factor to those where the internal biomass density was scaled instead.

It is clear from both columns of Figure 2 that either method described above compensated, to some extent, for the differences in biofilm structure caused by the different packing densities of circles and of spheres. The overall thicknesses of 2D biofilms grew at a more similar rate to that of an equivalent 3D biofilm when we adjust either the internal biomass density (Figure 2A) or the shove factor (Figure 2D). The specific growth rate profiles (Figure 2B,E) and

overall vertical biomass density profiles (Figure 2C,F) with height also bore more resemblance when these adjustments were made.

Representing three-dimensional reality with a two-dimensional model is a simplification that is often made for computational efficiency but, as with all such simplifications, modellers should beware unintended consequences. We have proposed two methods for counteracting the unintended consequence of higher packing density when moving from spheres (3D) to circles (2D), and shown that they yield more consistent simulation results. Both scaling methods perform equally well, so we do not recommend one over the other. This approach may also be useful to researchers making similar assumptions in other fields.

Conflict of interest statement

The authors declare that the research was conducted in the absence of any commercial or financial relationships that could be construed as a potential conflict of interest.

Acknowledgements

The authors are grateful to the UK National Centre for the Replacement, Refinement & Reduction of Animals in Research (NC3Rs) for funding their development of individual-based models (IBMs) for the gut environment (eGUT grant NC/K000683/1). All figures created using the package *matplotlib* (Hunter, 2007) in Python 2.7 (Python Software Foundation, 2010).

References

Ackermann, M., Schreiber, F., 2015. A growing focus on bacterial individuality. Environ. Microbiol. 17, 2193–2195.

Allison, D.G., Gilbert, P., 1992. Bacterial biofilms. Sci. Prog. 76, 305–321.

Alpkvist, E., Picioreanu, C., van Loosdrecht, M.C.M., Heyden, A., 2006. Three-dimensional biofilm model with individual cells and continuum EPS matrix. Biotechnol. Bioeng. 94, 961–979.

Ardré, M., Henry, H., Douarche, C., Plapp, M., 2015. An individual-based model for biofilm formation at liquid surfaces. Phys. Biol. 12, 66015.

Berryman, J.G., 1983. Random close packing of hard spheres and disks. Phys. Rev. A 27, 1053–1061.

Costerton, J.W., Lewandowski, Z., Caldwell, D.E., Korber, D.R., Lappin-Scott, H.M., 1995. Microbial biofilms. Annu. Rev. Microbiol. 49, 711–745.

Gunawardena, J., 2014. Models in biology: "accurate descriptions of our pathetic thinking." BMC Biol. 12, 29.

Hales, T.C., 1992. The sphere packing problem. J. Comput. Appl. Math. 44, 41–76.

Hellweger, F.L., Clegg, R.J., Clark, J.R., Plugge, C.M., Kreft, J.-U., 2016. Advancing microbial sciences by individual-based modelling. Nat. Rev. Microbiol. 14, 461–471.

Horn, H., Lackner, S., 2014. Modeling of Biofilm Systems: A Review, in: Muffler, K., Ulber, R. (Eds.), Productive Biofilms, Advances in Biochemical Engineering/Biotechnology. Springer International Publishing, pp. 53–76.

Hunter, J.D., 2007. Matplotlib: a 2D graphics environment. Comput. Sci. Eng. 9, 90–95.

Kreft, J.-U., Booth, G., Wimpenny, J.W.T., 1998. BacSim, a simulator for individual-based modelling of bacterial colony growth. Microbiology 144, 3275–3287.

Kreft, J.-U., Plugge, C.M., Grimm, V., Prats, C., Leveau, J.H.J., Banitz, T., Baines, S., Clark, J., Ros, A., Klapper, I., Topping, C.J., Sinskey, A.J., Schuler, A., Litchman, E., Hellweger, F.L., 2013. Mighty small: Observing and modeling individual microbes becomes big science. Proc. Natl. Acad. Sci. U. S. A. 110, 18027–18028.

Lardon, L.A., Merkey, B.V., Martins, S., Dötsch, A., Picioreanu, C., Kreft, J.-U., Smets, B.F., 2011. iDynoMiCS: next-generation individual-based modelling of biofilms. Environ. Microbiol. 13, 2416–2434.

Lu, Y., Wang, Z., Chong, K., 2005. A comparative study of buried structure in soil subjected to blast load using 2D and 3D numerical simulations. Soil Dyn. Earthq. Eng. 25, 275–288.

Manz, B., Volke, F., Goll, D., Horn, H., 2003. Measuring local flow velocities and biofilm structure in biofilm systems with magnetic resonance imaging (MRI). Biotechnol. Bioeng. 84, 424–432.

Neu, T.R., Manz, B., Volke, F., Dynes, J.J., Hitchcock, A.P., Lawrence, J.R., 2010. Advanced imaging techniques for assessment of structure, composition and function in biofilm systems. FEMS Microbiol. Ecol. 72, 1–21.

Picioreanu, C., Kreft, J.-U., van Loosdrecht, M.C.M., 2004. Particle-based multidimensional multispecies biofilm model. Appl. Environ. Microbiol. 70, 3024–3040.

Picioreanu, C., van Loosdrecht, M.C.M., Heijnen, J.J., 1998a. A new combined differential-discrete cellular automaton approach for biofilm modeling: application for growth in gel beads. Biotechnol. Bioeng. 57, 718–731.

Picioreanu, C., van Loosdrecht, M.C.M., Heijnen, J.J., 1998b. Mathematical modeling of biofilm structure with a hybrid differential-discrete cellular automaton approach. Biotechnol. Bioeng. 58, 101–116.

Python Software Foundation, 2010. Python: Version 2.7.

Tóth, L.F., 1972. Lagerungen in der Ebene auf der Kugel und im Raum. Springer Berlin Heidelberg, Berlin, Heidelberg.

Visscher, W.M., Bolsterli, M., 1972. Random packing of equal and unequal spheres in two and three dimensions. Nature 239, 504–507.

Wanner, O., Eberl, H.J., Morgenroth, E., Noguera, D.R., Picioreanu, C., Rittmann, B.E., Van Loosdrecht, M.C.M., 2006. Mathematical modeling of biofilms. IWA Publishing, London.

Woodard, J.C., Dunatunga, S., Shakhnovich, E.I., 2016. A simple model of protein domain swapping in crowded cellular environments. Biophys. J. 110, 2367–2376.

Figure legends

Figure 1. Biofilm simulations. (A,B) Typical biofilm structures simulated using the parameters given in **Supplementary File 2**. Cells are shown in red and the solute concentration in greyscale: white for the maximum concentration in the bulk liquid (c_b, 1 mg L^{-1}) and black for no solute (0 mg L^{-1}). The solid surface is shown as a black region at the bottom of each panel. **(A)** is three-dimensional; **(B)** two-dimensional, using the unscaled values of ρ and s_f.

Figure 2. Simulation results confirm success of compensation measures. Three-dimensional simulations are shown in black, un-scaled two-dimensional simulations in red, and scaled two-dimensional simulations in blue. All panels show results of triplicate sets of simulations for each colour, where only the random seed differs between simulations. **(A-C)** Aggregated results for simulations where the cell internal biomass density, ρ, is adjusted. **(D-F)** Aggregated results for simulations where the shove factor, s_f, is adjusted. **(A,D)** Maximum biofilm thickness through time. **(B,E)** Specific growth rate of cells against height above the solid surface. **(C,F)** Average overall biomass density against height above the solid surface; each average is over a bin of width h = 2μm. The fluctuations are smaller in 3D (black) as the results are averaged over a larger system than in 2D (red and blue). **(B,C,E,F)** Snapshots shown at end of simulation, i.e. where the maximum thickness, T_{max}, is reached (see Supplementary Table 1).

Figure 3. Shove factor. (A) For the purposes of the shoving algorithm, the radii of the cells are scaled by a shove factor, s_f. This means that a small overlap between cells of these scaled radii (dotted lines) can be permitted for computational efficiency, without risking overlap of the actual cells (solid lines). **(B-C)** As the shove factor increases, the packing density of cells decreases. Results are shown for 2D **(B)** and for 3D **(C)**: simulation results (black crosses) lie below the theoretical maximum packing density (solid red line), but slightly above the theoretical packing density for random close packing (dashed red line).

Supplementary files

Supplementary File 2. Supporting information. Simulation description and parameters, and notes on packing density.

Supplementary File 3. Source code, protocol files, and analysis scripts used. Simulations can be run on a standard desktop computer overnight. Java™ 1.8 is required. *.zip* file (9MB).

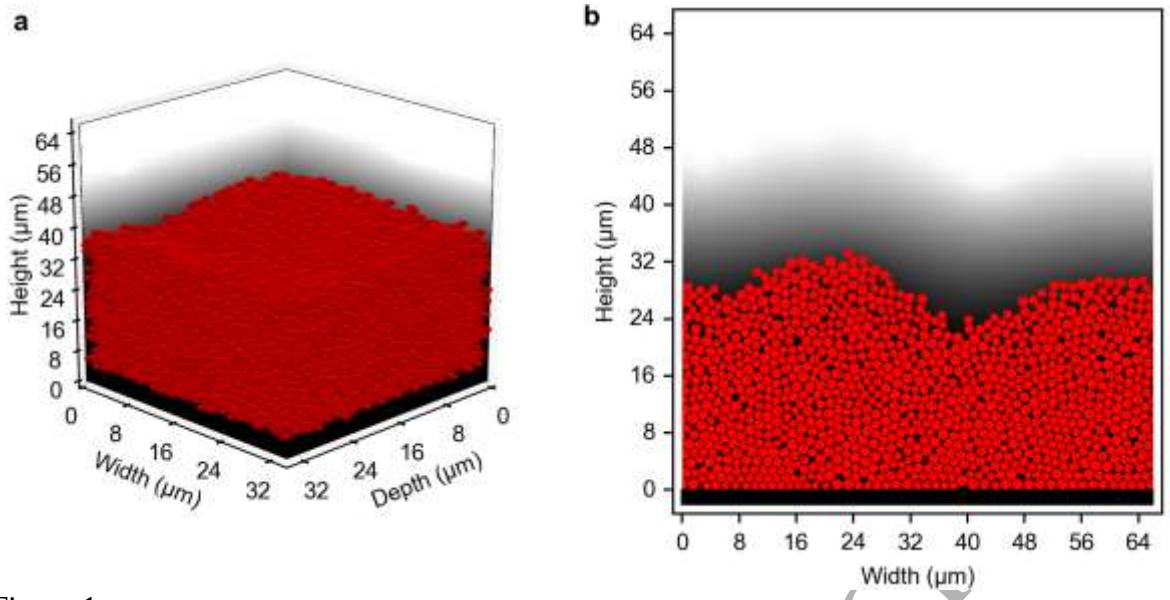

Figure 1

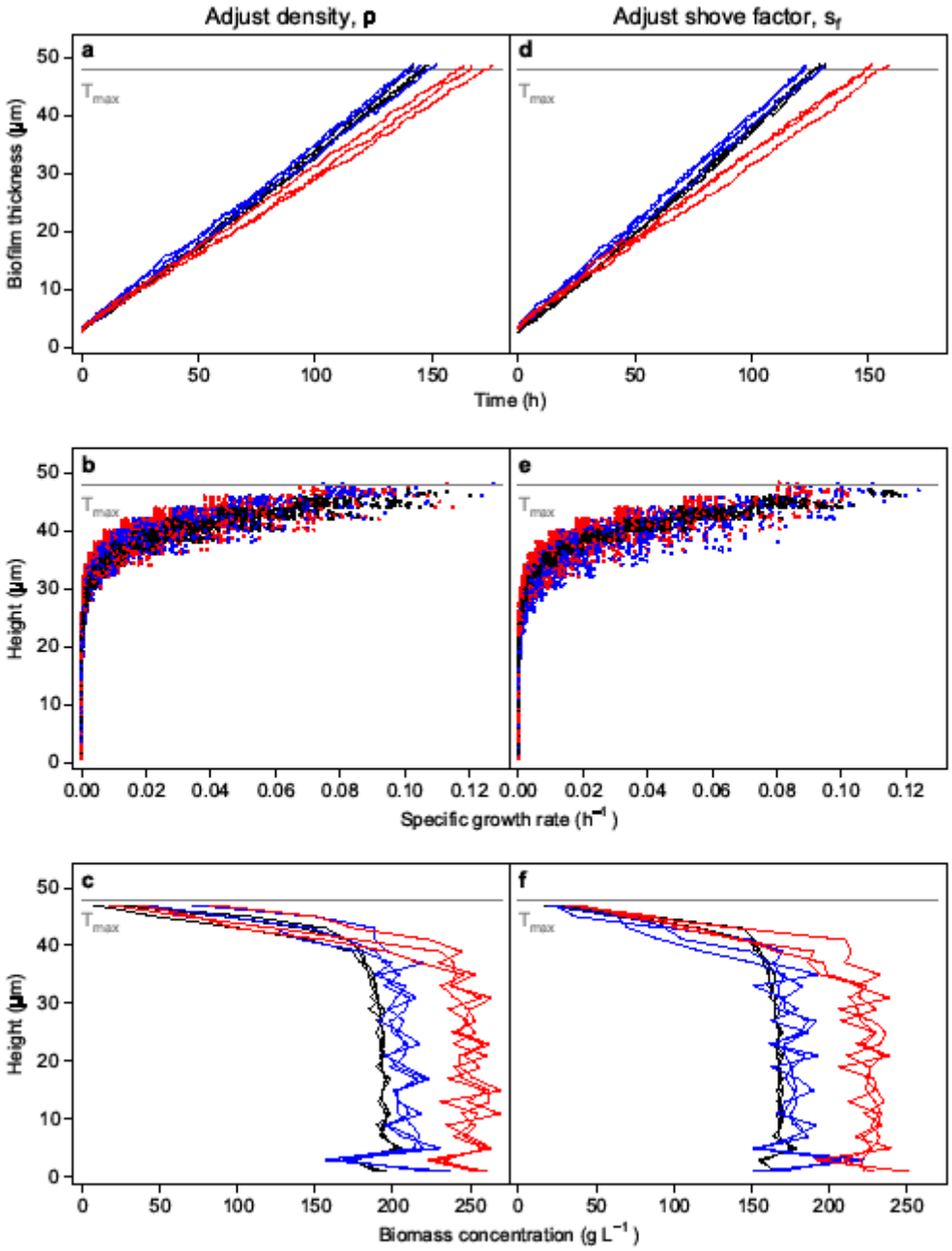
Adjust density, ρ
Adjust shove factor, s_f
a
d
b
e
c
f
T_{max}
Biofilm thickness (μm)
Height (μm)
Time (h)
Specific growth rate (h^{-1})
Biomass concentration ($g\ L^{-1}$)

Figure 2

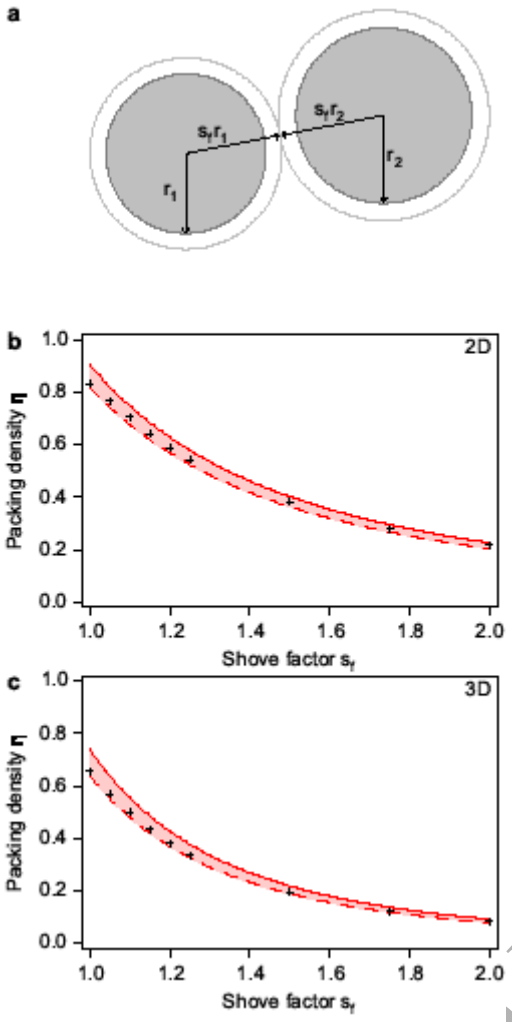

Figure 3